ELSEVIER

Physics of the Earth and Planetary Interiors 119 (2000) 259–267

PHYSICS OF THE EARTH AND PLANETARY INTERIORS

www.elsevier.com/locate/pepi

Hematite vs. magnetite as the signature for planetary magnetic anomalies?

Günther Kletetschka *, Peter J. Wasilewski, Patrick T. Taylor

NASA Goddard Space Flight Center, Greenbelt, MD 20771, USA

Received 25 August 1999; accepted 8 December 1999

Abstract

Crustal magnetic anomalies are the result of adjacent geologic units having contrasting magnetization. This magnetization arises from induction and/or remanence. In a planetary context we now know that Mars has significant crustal magnetic anomalies due to remanent magnetization, while on the Earth both remanence and induction can contribute to the magnetic anomaly, because of the presence of the Earth's magnetic field. If there is a significant induced magnetization (IM) then magnetite is commonly assumed as the source, since it has a much greater magnetic susceptibility, when compared with other magnetic minerals.

We investigated the thermoremanent magnetization (TRM) acquisition of hematite to determine if the remanent and induced magnetization of hematite could compete with magnetite in weak magnetic fields up to 1 mT. TRM acquisition curves of magnetite and hematite show that multidomain hematite approaches TRM saturation (0.3–0.4 A m^2/kg) in fields as low as 0.1 mT. However, multidomain magnetite reaches only a few percent of its TRM saturation in a field of 0.1 mT (0.02–0.06 A m^2/kg). These results suggest that a mineral such as multidomain hematite and, perhaps, other minerals with significant remanence and minor induced magnetization may play an important role in providing requisite magnetization contrast. Consequently, we should reevaluate where multidomain hematite exists in significant concentration, allowing a better insight into the role of remanent magnetization in the interpretation of the magnetic anomalies.

Keywords: Hematite; Magnetite; Magnetic anomalies; Magnetic remanence; Induced magnetization; Thermoremanent magnetization; Magnetic susceptibility; TRM; Remanence acquisition; Hematite morphology; Hysteresis properties; Coercivity; National Museum of Natural History; REM; SIRM; Saturation isothermal remanent magnetization; Mixtures

1. Introduction

We consider two assumptions in this report central to the interpretation of large amplitude continental magnetic anomalies which likely have their sources in mid to deep levels of the crust. (1) Main magnetic mineral is magnetite, and (2) in the case of the continental Earth the mode of magnetization is entirely induction.

Generally when someone considers how ''magnetic'' something is he or she may use a strong magnet to test for the attraction force between the magnet and the object. The strong magnet is a source

* Corresponding author. Tel.: +1-301-286-3804; fax: +1-301-286-0212.

E-mail address: gunther@denali.gsfc.nasa.gov (G. Kletetschka).

0031-9201/00/$ - see front matter
PII: S0031-9201(00)00141-2

of strong inducing field that is 3–5 orders of magnitude more intense than the intensity of the geomagnetic field. This procedure will raise the induced magnetization (IM) of the object (for example a rock with magnetite particles) 3–5 orders of magnitude, or in case of a very strong magnet towards the saturation point of the magnetic carriers. When attraction is observed it is most likely due to magnetite, which has a large induction because of its large magnetic susceptibility. The large values of induced magnetization exhibited by MD magnetite are responsible for the common belief that magnetite is the likely source of terrestrial crustal magnetic anomalies (Shive and Fountain, 1988; Wasilewski and Mayhew, 1992).

Clark (1983) summarized the range of thermoremanent magnetization (TRM) expected for the principal iron oxide minerals found in terrestrial rocks. Insofar as we are aware (McSween, 1985) the same iron oxide mineralogies are found in the Martian rocks. Magnetic properties of iron oxide minerals change according to their grain size. The critical single domain size for magnetite is 0.05–0.084 μm, for hematite the size is 15 μm, for titanomagnetite the size is 0.2–0.6 μm, and for pyrrhotite the size is 1.6 μm (Dunlop and Özdemir, 1997, Table 5.1). Wasilewski and Warner (1994) used the SD–PSD–MD (Single Domain–Pseudo Single Domain–Multi Domain) categorization based on size dependent hysteresis properties (Day et al., 1977) and presented magnetic hysteresis data for a wide range of samples including xenoliths, high grade metamorphic terrane, crustal sections, etc. This SD–PSD–MD categorization suggests that most rocks contain PSD–small MD grains.

Part of this paper reiterates the Clark (1983) emphasis on the importance of remanence in magnetic anomaly interpretation. Magnetite, titanomagnetite, and pyrrhotite, all of which are found in the SNC meteorites (McSween, 1985), and MD hematite (Christensen et al., 2000), should be considered as possible candidates for the large planetary magnetic signatures. Maghemite if present would be magnetically similar to magnetite (Dunlop and Özdemir, 1997).

2. Magnetization of hematite and magnetite

The most common terrestrial magnetic iron oxide is magnetite (Fe_3O_4). In the Earth's field (0.05 mT) magnetite has the largest Induced Magnetization (60–220 A/m) among the common magnetic minerals (e.g., Maher, 1988). Induced magnetization, M_i, is a function of magnetic susceptibility χ and the external magnetic field $\boldsymbol{H}$: ($M_i = \chi \boldsymbol{H}/\mu$), where μ ($\mu = 4\pi \times 10^{-7}$ Ω s/m) is the vacuum magnetic permeability). Magnetite can also exist in a superparamagnetic (SP) state when the grain size is smaller than 50 nm. Under this condition the susceptibility of a 30-nm-size cube of magnetite, at room temperature, is about 650 (Dunlop and Özdemir, 1997) which produces an enormous induced magnetization of approximately 26,000 A/m.

A comparison of TRM of magnetite relative to its induced magnetization is given in Table 1. Schlinger

Table 1
Induced and thermoremanent magnetization is acquired in a presence of 50 μT external magnetic field

Magnetization of magnetite and hematite			
	Induced [A/m]	Thermoremanent [A/m]	Total [A/m]
Magnetite			
20–200 μm	~ 140 (Maher, 1988)	60–25 (Dunlop, 1990)	200–165
2–20 μm	80–140 (Maher, 1988)	250–60 (Dunlop, 1990)	330–200
0.2–2 μm	60–80 (Maher, 1988)	1000–250 (Dunlop, 1990)	1060–330
0.02–0.2 μm	220–60 (Maher, 1988)	5000–1000 (Dunlop, 1990)	5220–1060
0–0.02 μm	26,000 (Dunlop and Özdemir, 1997)	0	26,000
Hematite			
20–200 μm	~ 7 (this study)	600–1600 (this study)	600–1600
0–20 μm	0.02–2 (Hunt et al., 1995)	30–300 (Clark, 1983)	30–300

(1985) suggested that the most common range of magnetite grain size is 20–200 μm for mid and deep crustal rocks. This 20–200 μm grain size range gives TRM values, in crustal conditions, of 25–250 A/m (Dunlop, 1990). Taking into account magnetite susceptibilities for these grain sizes (Maher, 1988) we have induced magnetization between 80 and 140 A/m (see Table 1). This indicates that in the geomagnetic field a magnetite-rich rock, with acquired thermoremanence, may have significantly larger remanent than induced magnetization. The relative significance of induced and remanent magnetization is expressed by their ratio known as Koenigsberger ratio (Q). Data in Table 1 indicates that Q should be generally greater than one for both hematite and magnetite. This is not true in cases where the original thermoremanence was destroyed (chemically and/or physically) or when different types of remanence have been re-acquired (for review see Table 3.1 in Merrill et al., 1996). For example, the introduction of superparamagnetic particles of magnetite, due to various types of chemical alteration of iron silicates, could be significant but is probably not common because the volume of coarse-grained magnetite in rock is usually much greater than the volume of superparamagnetic magnetite.

The second most abundant iron oxide found in crustal rocks is hematite (Fe_2O_3). Hematite as well as other common iron bearing minerals has susceptibility less than 0.01 SI. This would mean, that the total induced magnetization of a hematite–magnetite bearing rock is dominated almost entirely by magnetite (see Tables 1 and 3). Would its remanent magnetization dominate the total magnetization of a rock where both minerals are present and hematite is significant volumetrically?

To investigate this scenario hematite specimens were obtained from all over the world (selected from the mineral collection in the National Museum of Natural History, Smithsonian Institution, Washington

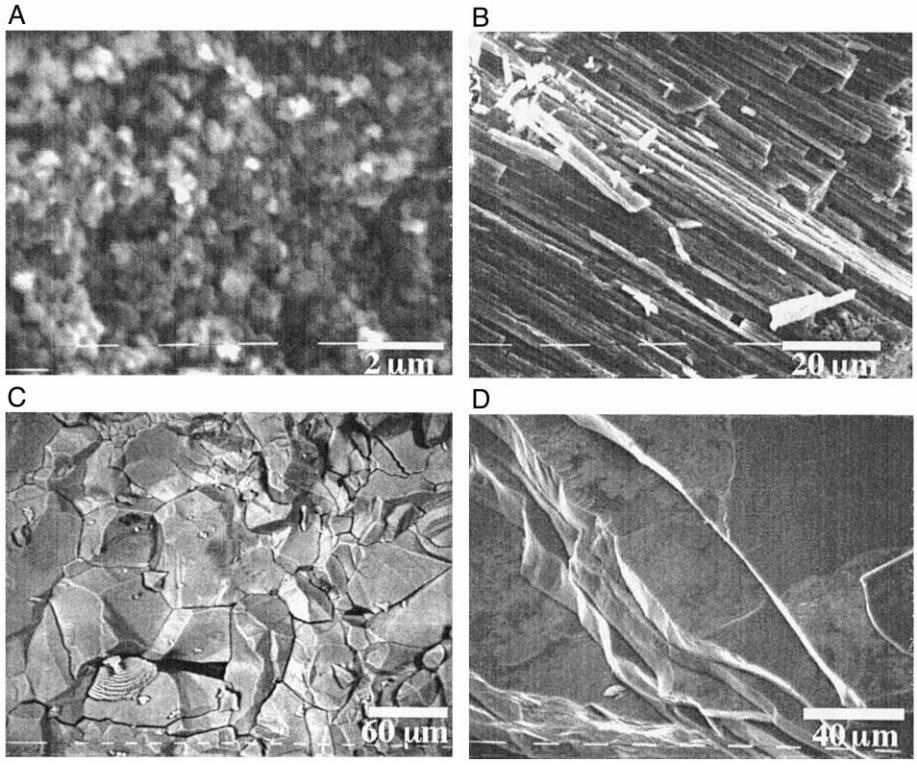

Fig. 1. Four common forms of hematite: (A) fine-grained reddish powder (N114078); (B) pencil-like (N13026); (C) equidimensional coarse-grained (NR17174); (D) plate like (N36085).

DC). The specimens from the Smithsonian collection could be divided into four groups (Fig. 1). The first group consists of compact fine powder of reddish hematite with grain size less that 1 μm (See Fig. 1). The second group is made up of pencil-shaped rods, with the pencil-cross-sectional diameter between 0.2 and 3 μm. The third group contains equidimensional, shiny, coarse grains (> 60 μm). The forth group consists of thin plates where the plate thickness varies from 0.1 to 10 μm.

3. Experimental procedures

Samples were characterized by X-ray diffraction, Curie temperature and saturation magnetization. X-ray diffraction analysis confirmed the high purity of the coarse-grained hematite grains as no other phase was detected. X-ray analyses of fine powdered hematite revealed quartz particles but no magnetite. The absence of magnetite is also indicated by the measured values of saturation magnetization (J_s), which ranged between 0.2 and 0.5 A m^2 kg^{-1} (see Table 2). If these samples would be contaminated by magnetite, Js would be larger than the listed value for J_s of hematite ($\sim$ 0.4 A m^2 kg^{-1} in Hunt et al., 1995). The titanium component was not detected during the Curie temperature measurements, which confirmed the temperature for pure hematite (670°C).

Morphological study was done by scanning electron microscopy on non-coated samples chipped off the USNM specimens. We used the Philips SEM 500M operating at 25 kV accelerating voltage and spotsize of 320 Å. Representative morphologies are depicted in Fig. 1.

Magnetic measurements were made on small pieces (about 50 mm^3) from the original USNM samples. The mixture of 8 parts of ceramic adhesive (item #919, made by Cotronix) and 1 part of water was used to attach samples to the circular 1 inch glass slide. Natural Remanent Magnetization (NRM) values of slides were measured with the Superconducting Rock Magnetometer (SRM, Superconducting technology).

Slides used in the NRM measurements were attached to the end of plastic rod by means of nonmagnetic double-stick scotch tape and measured with the vibrating sample magnetometer (VSM), Lake Shore model 7300. The magnetic field was supplied by a large water cooled 12-in. Varian magnet, driven by a Tidewater bipolar power supply. The maximum field was 2 T. Representative hysteresis loops are shown

Table 2
Most of the samples of hematite are from Smithsonian Institution, Department of Mineral Sciences (USNM). Sample L2 is a representative sample from an old iron mine near Fire Lake in Central Labrador, Canada, collected for the University of Minnesota (UofM) study (Kletetschka and Stout, 1998). Sample 90LP12 contains coarse crystals of non-titanium magnetite obtained from Prof. John Valley, University of Wisconsin (UofW). Hysteresis parameters: Saturation magnetization (J_s), Saturation Isothermal Remanent Magnetization (SIRM), Coercivity field (H_c)

Samples of hematite and magnetite

Sample	Origin morphology	J_s [A m^2 kg^{-1}]	SIRM [A m^2 kg^{-1}]	H_c [T]
N115249	USNM, Brazil Coarse-grained hematite	0.392	0.214	0.013
NR17174	USNM, Arizona Coarse-grained hematite	0.468	0.350	0.008
L2	UofM, Labrador Coarse-grained hematite	0.420	0.230	0.004
N114078	USNM, Iran Fine-grained hematite	0.466	0.346	0.260
B7379	USNM, Germany Fine-grained hematite	0.256	0.176	0.464
No115380	USNM, Egypt Fine-grained hematite	0.200	0.116	0.222
N66844	USNM, Germany Pencil-like hematite	0.324	0.316	0.329
N13026	USNM, Germany Pencil-like hematite	0.328	0.302	0.411
NR13597	USNM, England Pencil-like hematite	0.288	0.272	0.764
B7371	USNM, Michigan Plate-like hematite	0.436	0.346	0.053
N127244	USNM, Greenland Plate-like hematite	0.122	0.096	0.076
N36085	USNM, England Plate-like hematite	0.382	0.312	0.066
N46422	USNM, Africa Plate-like hematite	0.498	0.346	0.069
90LP12	UofW, Adirondacks Coarse grained magnetite	82.4	1.922	0.001

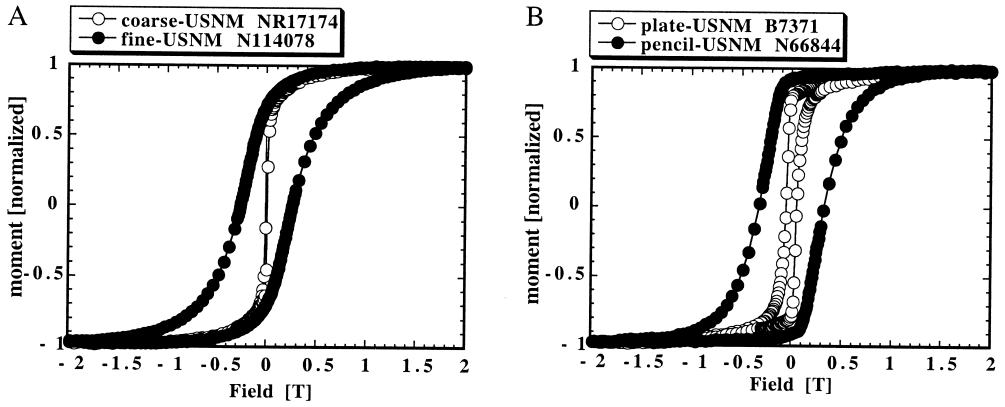

Fig. 2. Different morphology of hematite is reflected in the shape of the hysteresis loops. (A) fine-grained and coarse-grained. (B) plate-like and pencil-like.

in Fig. 2 and hysteresis parameters of all samples are in Table 2.

A fine-grained sample (N114078-grain size estimated from the SEM observation as about 1 μm, see also Fig. 1A) and a coarse grained one (N17174-part of a single crystal about 5 mm in diameter) were used to demonstrate magnetic behavior of coarse and fine grained samples. Data for the coarse and fine-grained hematite samples can be found in Figs. 1–4 and Table 2. No superparamagnetic particles in the fine-grained hematite samples were detected due to the observational absence of a constricted shape of the hysteresis loops (Wasilewski, 1973) and the large ratio of saturation remanence to saturation magnetization (SIRM/J_s, see Table 2).

Isothermal remanence acquisition (IRM) curves are useful in that they reflect the coercivity of the material in question and in fact are related to the various high field characterization techniques that are presently in use (Denkers, 1981). IRM acquisition curves were determined with the VSM. After finishing magnetic hysteresis measurements the samples were demagnetized by application of an appropriate reversed field (coercivity of remanence). Samples were iteratively DC demagnetized in a VSM until the remanence was zero at zero field. The programmed excursions applied magnetic field steps whereafter the remanence would be measured after the applied field was reduced to zero. The field steps were programmed up to 2 T.

The TRM acquisition curves are acquired in controlled weak fields for the purpose of investigating the intensity of TRM that could be acquired over a

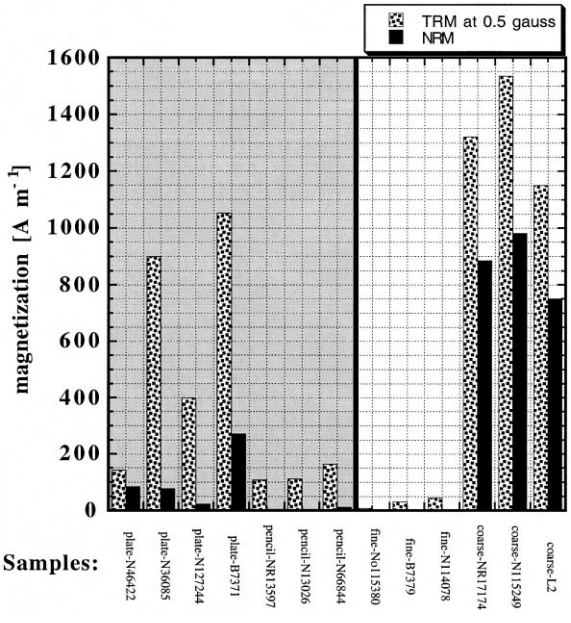

Fig. 3. Magnetization of representative hematite samples characterizing the most common morphology. The anisotropic plate and pencil shaped samples are located in the shaded area. Sample numbers are those of the Department of Mineral Sciences, NMNH, Smithsonian Institution. Sample L2 is a coarse-grained hematite sample from Iron mine near Fire Lake in Central Labrador, Canada.

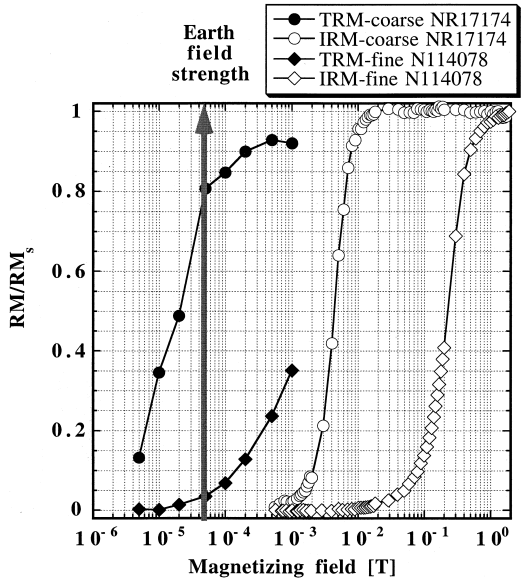

Fig. 4. Thermal (TRA) and isothermal (IRA) remanence acquisition curves for coarse and fine-grained hematite. Note that multidomain hematite is nearly saturated by the Earth's field. TRM acquisition of fine-grained hematite did not achieve saturation due to limited magnetizing field of the cooling chamber.

range of weak fields realistic for planetary bodies with possible dynamo generated fields less than or greater than the geomagnetic field. TRM acquisition experiments were done in a Schonstedt Thermal Demagnetizer cooling from a maximum temperature of 700°C for all samples. The oven was equipped with a cooling chamber containing a conducting coil, which can be used to produce an axial magnetic field during the cooling process. We applied a current through this conducting coil using a Lambda Power Supply. The magnetic field inside the cooling chamber was measured with a Gaussmeter (Bell model 620Z). The probe of this Gaussmeter was bent to fit inside the cooling chamber. Because the probe was modified we tested this gaussmeter against a Schonstedt Digital Magnetometer to ensure the calibration of magnetic field values. The fields applied during the cooling of our samples ranged from 0.005 to 1 mT. The smallest field inside this shielded oven was 0.002–0.003 mT. Consequently, we were not able to completely thermally demagnetize the coarse-grained hematite (NR17174) due to this residual magnetic field (0.002–0.003 mT) inside the shielded oven. The maximum acquisition field inside this shielded oven was 1 mT. The fine-grained hematite reached only about 40% of its SIRM, even when cooled in the maximum allowable 1-mT magnetic field. Hysteresis properties were measured before and after the thermal treatment to insure that the heating in air did not significantly change the characteristics of the mineralogy of our samples.

The mixtures of coarse-grained hematite and magnetite were prepared by reducing the size of the pure minerals (hematite N115249, magnetite 90LP12) down to about 0.5-mm equidimensional grains. Grains were picked from crushed samples. Each of the mixtures contained a total of 20 grains of oxide mineral. These grains were mixed and weighted and produced 25–30 mg of each oxide mixture. Separately, we mixed 8 parts of adhesive ceramic, Cotronix, item #919, and 1 part of water. We stirred each of our oxide mixtures into 0.05 cm^3 of ceramic material and poured the viscous substance into a small cylindrical opening (0.1 cm^3) in the center of a ceramic disc and let it solidify.

4. Results and discussion

Four different morphological groups of hematite show distinct magnetic hysteresis properties (Fig. 2). Results show (see Table 2) that coarse-grained hematite has relatively low coercivity (4–13 mT) and relatively large saturation remanence (0.21–0.35 A m^2 kg^{-1}). Fine-grained hematite has comparable saturation remanence (0.11–0.35 A m^2 kg^{-1}), however, the coercivity of these samples is much larger (220–460 mT). Both plate and pencil-like hematite grains have saturation remanence to saturation magnetization ratios close to unity. Plate-like hematite grains have a lower coercivity (66–76 mT) than the pencil-like ones (330–760 mT); this is probably due to the predominance of multiple domains in large planar grains and single domains in the pencil-like grains.

NRM and TRM values for the hematite used in this study are presented in the bar-graph form in Fig. 3 and Table 1. Both the SD powdered and pencil shaped samples have relatively small NRMs and TRMs (< 50 A m^{-1} for the fine powder and < 150

A m^{-1} for the pencil shaped). In contrast the plate like samples with NRMs up to 275 A m^{-1} can have TRMs up to 1000 A m^{-1}. The single crystal samples ($\sim$ 0.5 cm in diameter) have NRM's $>$ 750 A m^{-1} and the TRM's are $>$ 1000 and up to 1550 A m^{-1} and retain the largest percentage of the remanence over time (using the comparison of TRM and NRM).

Of all the natural magnetic minerals studied thus far only the coarse-grained hematite samples have a REM value (ratio between NRM and saturation remanence) much greater than 0.1. Previously large REM values were considered to be associated with contamination or with lightning strikes (Wasilewski and Kletetschka, 1999). These data on MD hematite refine our understanding about remanence in rocks. Hereafter, the large REM values might be associated with a possible MD hematite source.

The IRA curves for fine and coarse-grained hematite are shown in Fig. 4. The magnetic field required to achieve 50% saturation remanence is 0.005 T for the coarse hematite and 0.2 T for the fine hematite sample. These acquisition curves are consistent with the coercivities (see Fig. 2 and Table 2).

However, the TRA curves for the same samples (Fig. 4) show that for the fine grained hematite we need magnetic fields of tens of millitesla. For the coarse-grained hematite a surprisingly small hundreds of microtesla fields are enough to approach the SIRM of this sample. Therefore, even when cooling in a field as small as the geomagnetic field we can obtain a remarkable TRM, which is 60–80% of the saturation IRM (Fig. 4). An important feature of this MD hematite acquisition is that we can have a TRM, equivalent to that of magnetite, by a mineral with only a fraction of the saturation magnetization of magnetite. This may be a very relevant consideration for crustal magnetization models, particularly for Mars (Connerney et al., 1999).

The thermal behavior of the MD hematite seems to conflict with MD theory since MD hematite grains acquire a greater TRM than SD grains. According to the theory, however, TRM should be lower for MD grains because of domain interactions. Also the magnetic fields at which TRM reaches saturation should be inversely proportional to the SIRM (Dunlop and Özdemir, 1997). This seeming contradiction with the theoretical consideration can be explained by the difference between the magnitudes of the internal demagnetizing field for MD magnetite and MD hematite. In MD magnetite grains TRM can not saturate in a small magnetic field because of the opposition of the internal demagnetizing field. The size of this internal demagnetizing field is proportional to $(J_s)^2$. Js for magnetite ($\sim$ 90 A m^2 kg^{-1}) is almost 200 times larger than J_s for hematite (0.4 A m^2 kg^{-1}). This suggests that during TRM acquisition in MD hematite the internal demagnetizing field is much less than magnetite and allows MD hematite to reach saturation in weak magnetic fields.

TRM acquisition curves for mixtures of coarse-grained hematite and magnetite are shown in Fig. 5. MD magnetite TRM is much lower than the TRM of MD hematite acquired in a 50 μT external magnetic field. For MD magnetite to match the remanence of coarse-grained hematite would require 25 times more of this coarse-grained mineral.

The TRM acquisition curves for pure hematite grains, Fig. 5, represent results for samples diluted in the nonmagnetic ceramic medium, done to lower possible effects due to interactions between the grains. The nature of TRM acquisition seems to be

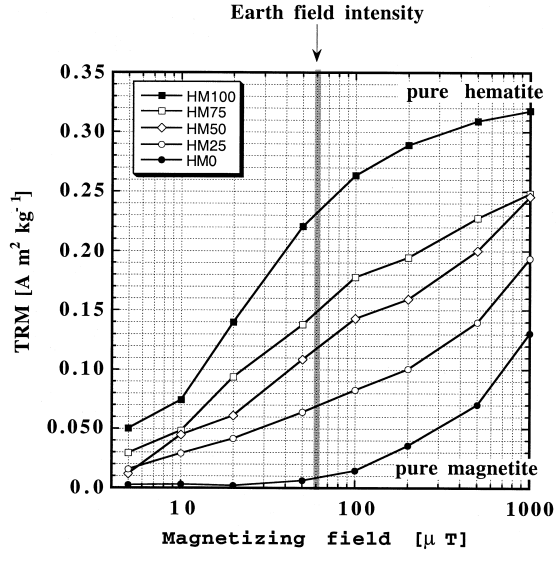

Fig. 5. Thermoremanent acquisition curves for artificial mixtures of coarse-grained hematite (HM100 = N115249) and magnetite (HM0 = 90LP12) randomly dispersed (grainsize $>$100 μm) in ceramic adhesive. Note that the TRM of magnetite grains is only about 4% of the TRM of just hematite grains in the Earth field during cooling. The exact proportions of hematite and magnetite are given in Table 3.

identical to the results shown in Fig. 4, where single crystals were measured, suggesting that any magnetic interaction effects in the mixtures were negligible.

5. Relevance to crustal magnetic anomalies

The relationship between induced and remanent magnetization for our artificial mixtures of hematite and magnetite is presented in Table 3. All of the hematite–magnetite mixtures have a greater TRM than induced. Assuming only multidomain magnetite to be the magnetic carrier, modeling gives us almost an order of magnitude lower magnetization than if the rocks contained the same amount of mutlidomain hematite. To illustrate this by an example, using our experimental data (Table 3), rock with 1% of multidomain magnetite would have magnetization $(40 + 190)\ A/m \times 0.01 = 2\ A/m$. Rock with 1% of multidomain hematite generates magnetization $(1165 + 7)\ A/m \times 0.01 = 12\ A/m$. Rocks with 1% of equal amounts of the two magnetic minerals have $(590 + 109)\ A/m \times 0.01 = 7\ A/m$. Magnetization of this magnitude ($7\ A/m$) is required by some of the magnetic anomaly models (Mayhew and LaBrecque, 1987; Mayhew et al., 1985; Shive et al., 1992).

If the oxygen fugacity and mineral composition allows hematite–magnetite assemblage to be formed, hematite minerals can provide dominant control over the distribution of magnetic anomalies by their TRM. This was the case in Canada, where Precambrian granulites, in Central Labrador, are enriched with Ti-hematite and where the oxygen fugacity during the metamorphism was relatively high (Kletetschka and Stout, 1995; Kletetschka, 1998). The magnetic anomaly in Central Labrador spans more than 5000 km^2 and is entirely due to concentration of hematite in the Wilson Lake allochthon (Kletetschka, 1998; Kletetschka and Stout, 1998).

Apart from the metamorphic terranes, the occurrence of coarse-grained hematite seems to be rather exceptional. Single domain behavior is more typical for sedimentary and chemically produced hematite. Such grains are typically $\ll 15\ \mu m$ in size. Because hematite grains up to $15\ \mu m$ in size are single domains (Dunlop and Özdemir, 1997, Table 5.1) their TRM acquisition potential is rather insignificant.

6. Conclusions

Our analysis of the remanent and induced magnetization of two major oxide minerals with very contrasting magnetic properties suggests that remanent magnetization may dominate induced magnetization regardless of the level of induced magnetization. Our results show that fine-grained hematite requires more than two orders of magnitude larger magnetizing field than coarse-grained hematite to achieve both IRM acquisition and TRM saturation. By comparing TRM acquisitions of coarse-grained hematite and magnetite we demonstrate that hematite may control the remanent magnetization, even if the rock contains an order of magnitude greater amount of magnetite than hematite.

Acknowledgements

We would like to thank our reviewer, David Dunlop, for contributing ideas regarding the origin of

Table 3
Magnetic measurements on various mixtures of hematite and magnetite favor coarse-grained hematite as the main carrier of total magnetization. M_i and TRM indicate induced and thermoremanent magnetization respectively in the Earth magnetic field. χ = susceptibility

Mixtures of hematite and magnetite						
Sample	Hematite [mg]	Magnetite [mg]	Total [mg]	TRM at 5×10^{-5} T [A/m]	Mass χ [m^3/kg]	M_i at 5×10^{-5} T [A/m]
HM100	25.3	0	25.3	1165	0.18	7
HM75	15.5	8.3	23.8	750	1.87	74
HM50	14.8	14.9	29.7	590	2.74	109
HM25	6.3	23.0	29.3	340	4.39	174
HM0	0	25.5	25.5	40	4.86	193

TRM in hematite. We acknowledge helpful comments of one anonymous reviewer. We wish to thank the Mineral Science Division of NMNH, Smithsonian Institution and Peter Dunn for his help with obtaining the hematite samples for this study. The X-ray diffraction studies were conducted by Chuan He of the GSFC.

References

Christensen, P.R., Clark, R.N., Kieffer, H.H., Kuzmin, R.O., Malin, M.C., Pearl, J.C., Bandfield, J., Edgett, K.S., Hamilton, V.E., Hoefen, T., Lane, M.D., Morris, R.V., Pearson, R., Roush, T.L., Ruff, S.W., Smith, M.D., 2000. Detection of localized crystalline hematite on mars from the thermal emission spectrometer investigation: evidence for near-surface water. Journal of Geophysical Research — Planets, in press.

Clark, D.A., 1983. Comments on magnetic petrophysics. Exploration Geophysics 14, 49–62.

Connerney, J.E.P., Acuña, M.H., Wasilewski, P.J., Ness, N.F., Reme, H., Mazelle, C., Vignes, D., Lin, R.P., Mitchell, D.L., Cloutier, P.A., 1999. Magnetic lineations in the ancient crust of Mars. Science 284, 794–798.

Day, R., Fuller, M.D., Schmidt, V.A., 1977. Hysteresis properties of titanomagnetites: grain size and compositional differences. Physics of the Earth and Planetary Interiors 13, 260–267.

Denkers, P., 1981. Relationship between median destructive field and remanent coercive forces for dispersed natural magnetite, titanomagnetite and hematite. Geophysical Journal of Royal Astronomical Society 64, 447–461.

Dunlop, D.J., 1990. Developments in rock magnetism. Reports Progress Physics 53, 707–792.

Dunlop, D.J., Özdemir, Ö., 1997. Rock Magnetism: Fundamentals and Frontiers. Cambridge Univ. Press, Cambridge, 573 pp.

Hunt, C.P., Moskowitz, B.M., Banerjee, S.K., 1995. Magnetic properties of rocks and minerals. In: Rock Physics and Phase Relations, A Handbook of Physical Constants. American Geophysical Union, pp. 189–203.

Kletetschka, G., 1998. Petrogenetic grids and their application to magnetic anomalies in lower crustal rocks. Labrador. PhD. Theses. University of Minnesota, 157 pp.

Kletetschka, G., Stout, J., 1995. Mössbauer analysis as a tool for deciphering the conditions of metamorphism. Journal of Czech Geological Society, Abstract 40, 23.

Kletetschka, G., Stout, J.H., 1998. The origin of magnetic anomalies in lower crustal rocks, Labrador. Geophysical Research Letters 25, 199–202.

Maher, B.A., 1988. Magnetic properties of some synthetic sub-micron magnetites. Geophysical Journal International 94, 83–96.

Mayhew, M.A., Johnson, B.D., Wasilewski, P.J., 1985. A review of problems and progress in studies of satellite magnetic anomalies. Journal of Geophysics Research 90, 2511–2522.

Mayhew, M.A., LaBrecque, J.L., 1987. Crustal geologic studies with magsat and surface magnetic data. Reviews of Geophysics 25, 971–981.

McSween, H.Y., 1985. SNC meteorites: clues to martian petrologic evolution? Reviews of Geophysics 23, 391–416.

Merrill, R.T., McElhinny, M.W., McFadden, P.L., 1996. The magnetic field of the earth, paleomagnetism, the core, and the deep mantle. In: Dmowska, R., Holtons, J.R. (Eds.), International Geophysics Series 63 Academic Press, 531 pp.

Schlinger, C.M., 1985. Magnetiation of lower crust and interpretation of regional magnetic anomalies: example from Lofoten and Vesteralen, Norway. Journal of Geophysics Research 90B, 11484–11504.

Shive, P.N., Blakely, R.J., Frost, B.R., Fountain, D.M., 1992. Magnetic properties of the lower continental crust. In: Fountain, D.M., Arculus, R., Kays, R.W. (Eds.), Continental Lower Crust. pp. 145–177.

Shive, P.N., Fountain, D.M., 1988. Magnetic mineralogy in an Archean crustal section: implications for crustal magnetization. Journal of Geophysics Research 93B, 12177–12186.

Wasilewski, P.J., 1973. Magnetic hysteresis in natural materials. Earth and Planetary Science Letters 20, 67–72.

Wasilewski, P., Kletetschka, G., 1999. Lodestone — natures only permanent magnet, what it is and how it gets charged. Geophysical Research Letters 26, 2275–2278.

Wasilewski, P.J., Mayhew, M.A., 1992. The Moho as a magnetic boundary revisited. Geophysics Research Letters 19, 2259–2262.

Wasilewski, P., Warner, R., 1994. The xenolith record: insights into the magnetic lithosphere. In: Magnetism: Rocks to Superconductors. Subbaraos, K.V. (Ed.), Geological Society of India, Memoir 29pp. 45–56.